Heat Transfer to Gas-Solids Suspensions Flowing Cocurrently Downward in a Circular Tube

Heat transfer to a gas-solids suspension flowing cocurrently downward in a 13-mm inside diameter tube with uniform heat-flux boundary conditions was investigated using 329-μm spherical glass beads in air. The gas Reynolds number varied from 0 to 30,000 with solids-loading ratios of up to 20 at a gas Reynolds number of 10,000. The suspension Nusselt number, defined in terms of the wall-to-gas mixed-mean temperature difference, decreased with increasing solids-loading ratio at high Reynolds numbers, while it changed little from the value for gas alone at low Reynolds numbers. A possible explanation is given by considering the effects of particles on the fluid mechanical properties of the gas. Asymptotic Nusselt numbers in downflow are compared with results of other investigations for upflow.

J. M. KIM and J. D. SEADER

Department of Chemical Engineering
University of Utah
Salt Lake City, UT 84112

SCOPE

The understanding of heat transfer to gas-solids suspensions is important in many chemical engineering processes such as pneumatic drying and cooling in gas-solid handling systems, catalytic cracking and reforming processes, and the combustion of pulverized coal. Further, it may play a primary role in designing transport coal conversion reactors in which the coal and hydrogen flow cocurrently downward through a tubular reactor while being heated through the tube wall (Ladelfa, 1977; Wood and Wiser, 1976). Due to a short residence time in transport reactors, the overall reaction rate would be greatly affected by transport phenomena, such as heat transfer and flow characteristics of the gas-solids suspension.

A number of investigations on the heat-transfer characteristics of flowing gas-solids suspensions have been conducted in the past. A significant increase in the heat-transfer coefficient by the addition of particles was reported in early papers by Farber and Morley (1957), Schluderberg et al. (1961), Farber and Depew (1963), and Wilkinson and Norman (1967). On the other hand, Abel et al. (1963), Briller and Peskin (1968), and Kane and Pfeffer (1973) observed no difference or rather a decrease in the heat transfer coefficient by adding particles. Depew and Farber (1963) and Tien and Quan (1962) reported the occurrence of a minimum Nusselt number for 30-μm glass bead-air suspensions at a solids-loading ratio of about 1.5. Nusselt numbers were found to be essentially unaffected by the addition of 200-μm particles up to a loading ratio, defined as particle flow rate to gas flow rate, of 7. A complicated behavior of the temperature profiles of the gas phase in the suspension was recently reported by Matsumoto et al. (1978).

Analytical attempts to treat suspension heat-transfer problems have suffered from a lack of knowledge and understanding about local motions of the suspension (Tien, 1961; Depew, 1960; Boothroyd, 1969). Chu and Depew (1972) introduced a thermal eddy diffusivity of the suspension, which was related to the momentum eddy diffusivity by the Reynolds analogy.

In spite of the extensive literature, large discrepancies among the results of different investigators are not fully accounted for, and prediction of the heat transfer rate to gas-solids suspensions is still a difficult problem (Boothroyd, 1971; Depew and Kramer, 1973). Further, most previous works were concerned with vertical-upflow or horizontal systems except for a recent paper by Wahi (1977), who studied the effect of test-section orientation on heat transfer for a limited range of solids-loading ratios.

The purposes of this study were to investigate local heat transfer characteristics of gas-solids suspensions in a cocurrent-downflow system using well-defined, closely sized glass beads in air, and to clarify the difference, if any existed, between the upflow and downflow cases by comparing the present data with those reported in the literature for the upflow system. Also the consequence of different Nusselt number definitions, which appears to be a source of confusion, was closely examined.

CONCLUSIONS AND SIGNIFICANCE

The thermal entry length is extended by the addition of particles and is more dependent on the solids-loading ratio than on the gas Reynolds number. At a gas Reynolds number of 9,800, the asymptotic Nusselt number, based on the gas mixed-mean temperature, stays almost constant at the value for gas alone for solids-loading ratios up to 20. However, it decreases with an increase in the solids-loading ratio at high Reynolds numbers. This is explained by considering opposing effects of particles on suspension heat transfer: boundary layer thinning which enhances the heat transfer, and reduced turbulence near the wall which inhibits the heat transfer. Although no increase in Nusselt number was found by the addition of particles, the total heat transfer rate from the wall to the suspension increased with solids-loading ratio because of increasing thermal capacity of suspensions.

Particle size has a large effect on the particle temperature attained in the heated tube. The temperature of 329-μm glass beads is much lower than the surrounding gas temperature. Therefore, Nusselt numbers based on suspension mixed-mean temperature may give erroneous conclusions about heat transfer mechanisms for coarse-particle suspensions. Comparison of the present data with upflow results shows that heat transfer processes of suspensions in downflow are weaker than in upflow.

Correspondence concerning this paper should be addressed to J. D. Seader. J. M. Kim is with C. F. Braun and Co., Alhambra, CA.

0001-1541-83-6705-0306-$2.00.

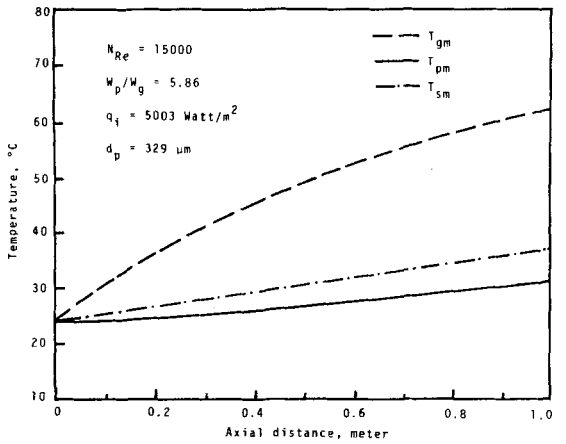

Figure 1. Gas and particle temperature profiles along the tube.

THEORETICAL BACKGROUNDS

For steady-state, one-dimensional suspension flow where viscous dissipation and radiation heat transfer between the wall and the particles are negligible, the thermal energy equations for a constant heat-flux boundary condition can be written as

$$U_g \frac{dT_{gm}}{dx} = \frac{4q_i}{\rho_g(1-E_p)C_{pg}D} - \frac{6h_pE_p}{\rho_g(1-E_p)C_{pg}d_p}(T_{gm}-T_{pm}) \tag{1}$$

$$U_p \frac{dT_{pm}}{dx} = \frac{6h_p}{\rho_pC_{pp}d_p}(T_{gm}-T_{pm}) \tag{2}$$

If the suspension flow is fully developed, with gas and particle temperatures equilibrated before the heat transfer test section, and the physical properties of the gas are assumed to be constant, Eqs. 1 and 2 reduce to linear equations with boundary condition,

$$T_{gm}(0) = T_{pm}(0) = T_i \tag{3}$$

Where $T_{gm}(0)$ and $T_{pm}(0)$ are the inlet temperatures of the gas and particles, respectively. Also, since Biot numbers for glass beads are generally smaller than 0.1, thermal gradients inside the particles can be neglected (Kreith, 1973). The solutions for gas and particle temperature yield

$$T_{gm}\{x\} = T_i + \frac{AB}{(A+C)}x + \frac{BC}{(A+C)^2}[1-e^{-(A+C)x}] \tag{4}$$

$$T_{pm}\{x\} = T_i + \frac{AB}{(A+C)}x - \frac{AB}{(A+B)^2}[1-e^{-(A+C)x}] \tag{5}$$

where

$$A = \frac{6k_gNu_p}{\rho_pC_{pp}U_pd_p^2}, \quad B = \frac{4q_i}{\rho_g(1-E_p)C_{pg}U_gD},$$
$$C = \frac{6k_gNu_pE_p}{\rho_g(1-E_p)C_{pg}U_gd_p^2}. \tag{6}$$

Thus, gas and particle temperatures can be evaluated using particle holdup and velocity data (Kim, 1979), and the particle Nusselt number correlation of Ranz and Marshall (1952). Solutions for a single particles case may be obtained by substituting $E_p = 0$ in Eq. 6.

For the case of a single particle, the temperature difference between the gas and the particle was calculated to be negligible for 30-μm particles; however, for the 329-μm particles that were used in this research, a substantial temperature difference existed, being about 25.6°C at the tube exit. Temperature profiles calculated at a typical experimental condition for the high solids-loading ratio is shown in Figure 1. The suspension mixed-mean temperature, T_{sm}, shown for comparison, is calculated by assuming that both phases attain thermal equilibrium at all axial locations, whence

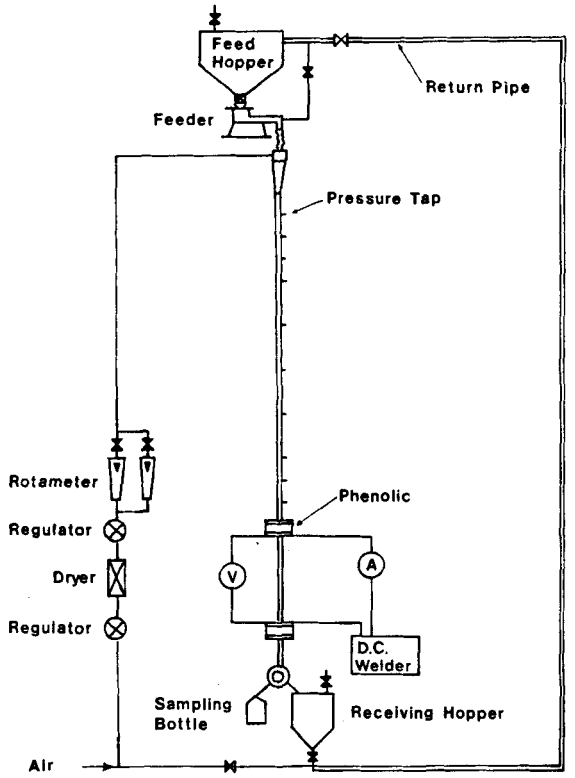

Figure 2. Overall heat transfer apparatus.

$$T_{sm}\{x\} = T_i + \frac{\pi Dq_ix}{W_gC_{pg}+W_pC_{pp}} \tag{7}$$

It is noted that, for the coarse particles employed in the present study, the suspension is far from thermal equilibrium with the gas at all axial locations.

Nusselt numbers for a suspension flow have been generally defined based on either the suspension mixed-mean temperature or the gas mixed-mean temperature as

$$Nu_s' = \frac{q_iD}{k_g(T_{wi}-T_{sm})} \tag{8}$$

or

$$Nu_s = \frac{q_iD}{k_g(T_{wi}-T_{gm})} \tag{9}$$

Figure 1 indicates, however, that the difference between Nu_s and Nu_s' would be substantial for 329-μm particles. If direct heat transfer from the wall to particles by radiation or conduction is negligible compared to convective heat transfer from the gas, heat transfer from the wall to the flowing suspension would be governed mainly by the fluid mechanical and thermal properties of the gas phase. Therefore, in the present research, the temperature potential between the wall and gas mixed-mean temperature was used to define the suspension Nusselt number. Further discussions on the consequences of different Nusselt number definitions will be presented in a later section.

EXPERIMENTAL

A schematic diagram of the apparatus used in this research is shown in Figure 2. The overall apparatus consisted of a gas and particle flow system, an approach section, and a heat transfer test section, which could be replaced with the holdup measurement section (Kim, 1979). The approach section, 13 mm in inside diameter and 6.7 m long, ensured hydrodynamically fully-developed conditions in the heat transfer test section. A 0.91-m-long heat transfer section was made of a type 304 stainless-steel seamless tubing with a 13-mm inside diameter and a 1.47-mm wall thickness. Since the tube was heated electrically, it was separated from the other sections by phenolic insulators. Copper flanges, silver-soldered at both ends of the tube, served as bus bars for electrical cables.

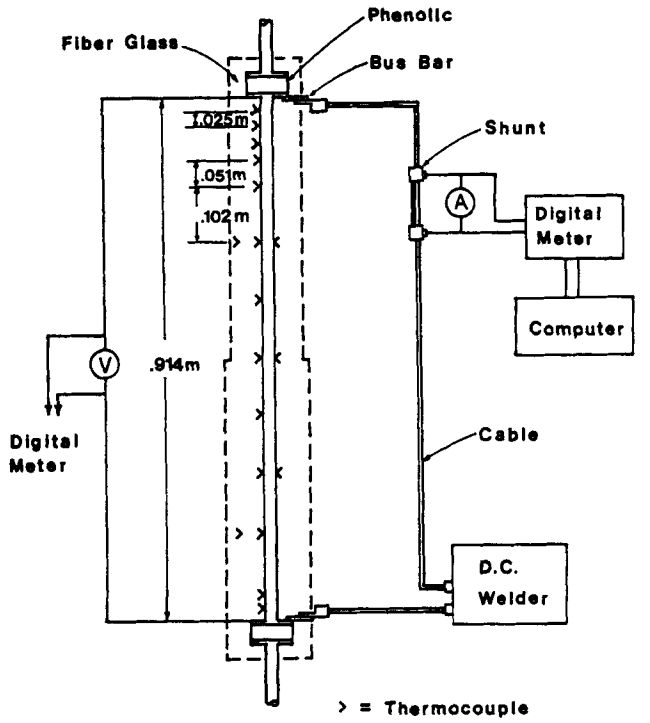

Figure 3. Detailed diagram of heat transfer test section.

Sixteen 30-gauge alumel-chromel thermocouples were installed on the outside surface of the tube at 13 axial locations. At three positions, the thermocouples were attached in pairs on opposite sides of the tube to check the uniformity of wall temperatures. The thermocouples were electrically insulated from the surface by mica sheets of approximately 0.025-mm thickness. The lead wires were wrapped tightly around the tube for two or three turns to minimize conduction losses near the junctions. The test section was then insulated with two layers of asbestos tape and 3.8-cm-thick fiberglass pipe insulation. Two sets of thermocouples were imbedded in the fiberglass insulation to serve as indicators for the long-term steady-state condition in the system. The location of the thermocouples are shown in Figure 3, where a detailed diagram of the test section and instrumentation are presented.

The thermocouple outputs were fed to a data logging system with 25 channels, which consisted of a Hewlett-Packard 3450A multifunction meter, a Cunningham scanner-control unit, a Hewlett Packard 5050B digital recorder, and a terminal panel. The data logger was then interfaced to a Wang 2200 Computer, which was programmed to scan all channels three to five times, and to average the readings for individual thermocouple outputs. The data were further processed by the computer with additional keyboard input data on the gas and particle flow rates. Inside surface temperatures of the tube were calculated from the equation given by Massier (1961) for heat transfer through the wall of a tube with electrical heat generation. Temperature gradients between the inside and outside tube wall, however, were generally negligible, ranging from 0.06 to 0.38°C.

A DC rectifier-transformer-type welder with a main current adjustment knob and a controller for fine adjustments, was used as the electric power supply. Voltage taps attached on the copper flanges at both ends of the heat transfer test section gave the voltage drop across the tube. The current was determined by measuring the voltage drop through a shunt connected in series with one of the electrical leads from the welder. The voltage taps from the tube and the shunt were also connected to the data logging system.

The particles used in this investigation were Ballotini soda lime glass beads with a density of 2.48 gm/cm^3. To obtain as closely sized particles as possible, the glass beads received from the manufacturer, which had a size range of minus 40/plus 50 mesh (US series), was further screened, yielding minus 45/plus 50 mesh glass beads for the tests. The average diameter of these beads was 329 μm. This diameter was the average of a sample of 130 glass beads measured under a microscope fitted with a micrometer eyepiece.

The system calibration runs were made using air alone; first, to check the performance of the apparatus and instruments, and secondly, to determine the heat loss correction to be applied to the measured electrical heat generation for the subsequent experiments with particles. Various air

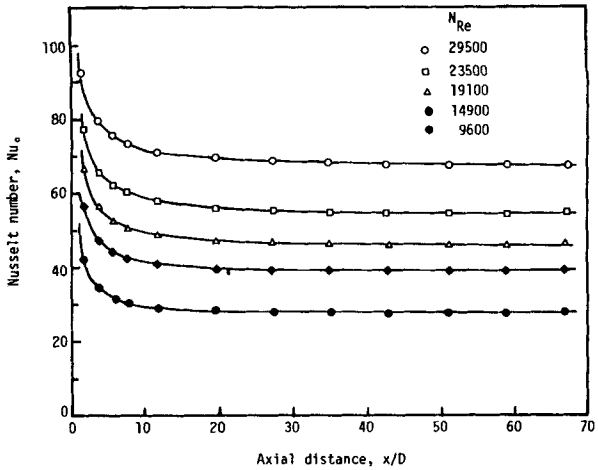

Figure 4. Local Nusselt numbers with flow of air alone.

flow rates were used, but at all times the outside tube wall temperature at the outlet was maintained at 121 ± 2.8°C to give constant heat loss through the insulation. During these runs, the inlet and outlet gas temperatures were measured to obtain the heat actually transferred to the flowing air stream. The heat losses were then determined by subtracting the heat transferred to the air from the generated heat in the tube wall. The average heat loss determined in this manner was 7.33 W which represented 3 to 8% of the total generated heat depending on the experimental conditions.

Experiments with suspensions were made by first setting the air flow rate and the electrical power at the desired level. When the system was stabilized, outputs from 23 thermocouples and 2-V taps were read five times and averaged for each channel by the computer. The processed results, in terms of 16 local Nusselt numbers with air alone, and the raw data were printed. On confirming consistent operation of the system by comparing these results with previous air calibration runs, particles were then added to the air stream. The electrical power was readjusted to keep the outlet tube wall temperatures at 121°C. The system reached steady state again in 10 to 15 minutes depending on the particle flow rate. Then the computer took all the readings as described above, and gave printouts of the results and raw data.

RESULTS AND DISCUSSION

Heat Transfer for Air Alone

Variation of local Nusselt number with dimensionless axial distance, x/D, is shown in Figure 4 for five different Reynolds numbers for the flow of air alone. In the entrance region, Nusselt numbers are large, but as expected they decrease rapidly to asymptotic values. The fully developed thermal condition exists for most of the tube section. Hence, the Nusselt number evaluated at the largest x/D of 67 can be regarded as an asymptotic Nusselt number. In Figure 5, experimental asymptotic Nusselt numbers are compared with the correlations of Kays and Leung (1963) and Sparrow et al. (1957), which are applicable to heat transfer with uniform heat-flux boundary conditions. The experimental results agree to ±5% with the equation of Kays and Leung (1963);

$$Nu_{0,\infty} = 0.022\, N_{Re}{}^{0.8} N_{Pr}{}^{0.6}. \qquad (10)$$

All the foregoing results for runs with air alone confirm reliability of the experimental system.

Heat Transfer for Suspension Flow

The Reynolds number for runs with air alone does not change at a fixed gas flow rate because physical properties of the air are evaluated at an average gas temperature of the inlet and outlet of the tube. In suspension heat transfer experiments, however, gas Reynolds number changes with the solids-loading ratio even at a fixed gas flow rate because the average of the inlet and outlet gas temperatures, at which physical properties are evaluated, is dif-

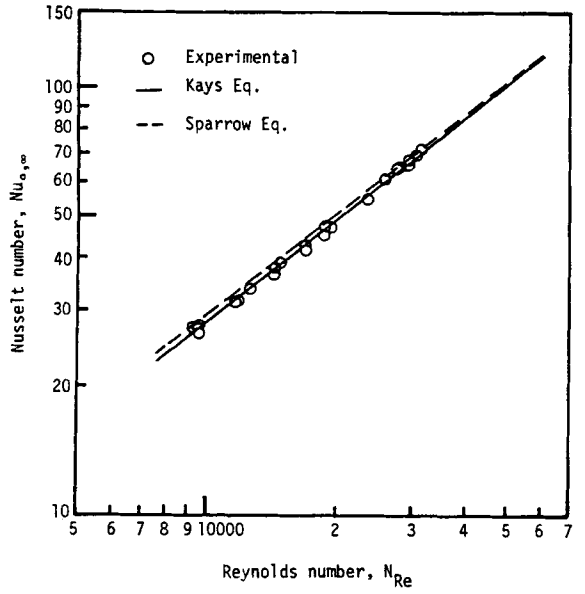

Figure 5. Asymptotic Nusselt numbers for flow of air alone.

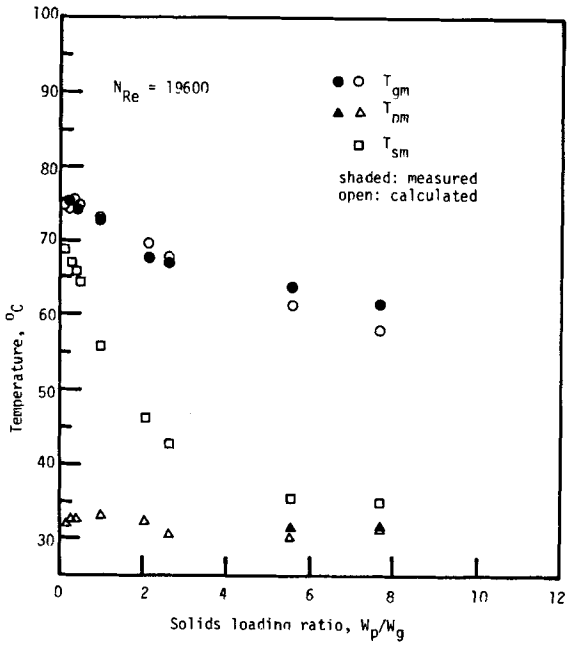

Figure 6. Comparison of calculated and measured temperatures.

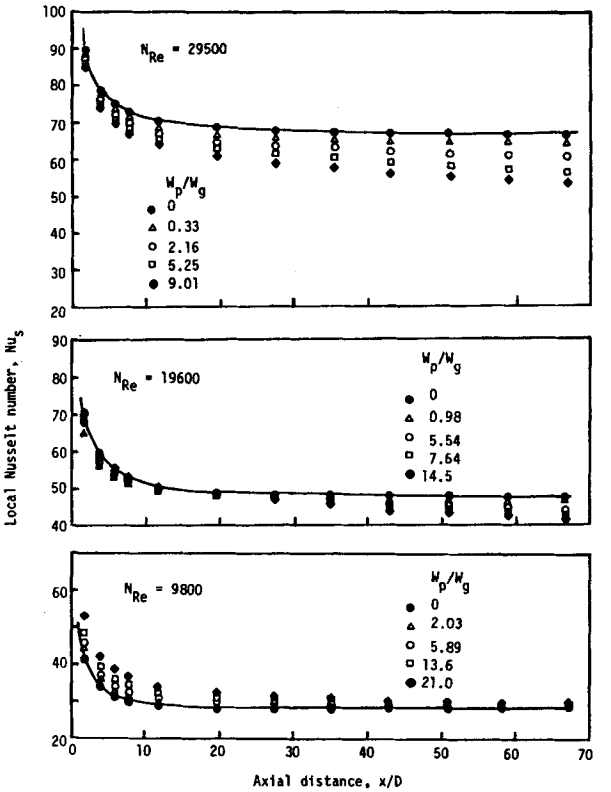

Figure 7. Effect of solids-loading ratio on local Nusselt number.

ferent for each loading. Because it was impractical to adjust gas flow rate to obtain the same Reynolds number for all runs, the gas Reynolds number used for suspension heat transfer experiments represents an average value of those for a series of runs at a fixed gas flow rate. However, gas Reynolds numbers for runs at a fixed gas flow rate differed less than 2% from the average value.

Accurate experimental measurement of the gas mixed-mean temperature involves determination of the radial gas temperature profile as well as the velocity profile at each axial position along the tube. However, in a suspension flow, determination of such profiles at one axial location alone presents enormous experimental difficulties even for very low solids-loading ratios. Hence, gas mixed-mean temperatures were calculated from Eq. 4. To check the adequacy of the calculated gas temperatures, several experimental measurements were made by inserting a thermocouple, shielded by stainless steel tubing, into the flow stream through the bottom phenolic connector. Radial variation of the temperature, as measured by changing the radial position of the thermocouple, was found to be less than 1.7°C, which generally represented 2% of the measured gas temperature. Hence, if heat transfer between the particles and thermocouple due to particle impact can be assumed to be negligible, which is reasonable at low loadings, this arrangement will measure approximate gas mixed-mean temperature. In addition to the gas-temperature measurements, the temperature of particles, collected in a sampling bottle by diverting the suspension flow at the three-way valve, was also measured with a glass thermometer.

The measured and calculated temperatures at the outlet of the tube are compared in Figure 6, where the calculated suspension mixed-mean temperatures are also shown for comparison. At low solids-loading ratios, the measured and calculated gas temperatures are in good agreement. Larger deviations are seen at high solids loadings; but the agreement is thought to be fairly good considering various unknown factors that can influence the temperature measurements. At high solids loadings, the measured and calculated particle temperatures seem to agree better than those of the gas. This is partly due to the small change in particle temperature while flowing in the heated tube. Note that suspension mixed-mean temperatures decrease rapidly up to a loading ratio of about 2 and that they are much lower than gas mixed-mean temperatures. It is concluded from Figure 6 that Eq. 4 predicts the gas mixed-mean temperature quite well. More importantly, the figure clearly shows that Nusselt numbers for a suspension would be greatly different depending on the choice of a temperature driving force. For example, the difference between gas mixed-mean temperature and suspension mixed-mean temperature is 25°C at a solids-loading ratio of 5.5 This would cause about a 50% variation in the total temperature potential, and hence the suspension Nusselt number.

Figure 7 shows the effect of solids-loading ratio on local Nusselt numbers along the axial distance for Reynolds numbers of 9,800, 19,600, and 29,500. The solid lines correspond to the flow of gas alone. Notice that variations in local Nusselt number with solids-loading ratio are different at low and high gas Reynolds numbers. At a Reynolds number of 9,800, Nusselt numbers in the entrance region increase somewhat with increasing solids-loading ratio, the effect being minimal near the tube end. Contrary effects of particles are observed however, at a Reynolds number of 29,500, where Nusselt numbers decrease with increasing solids-loading ratio for

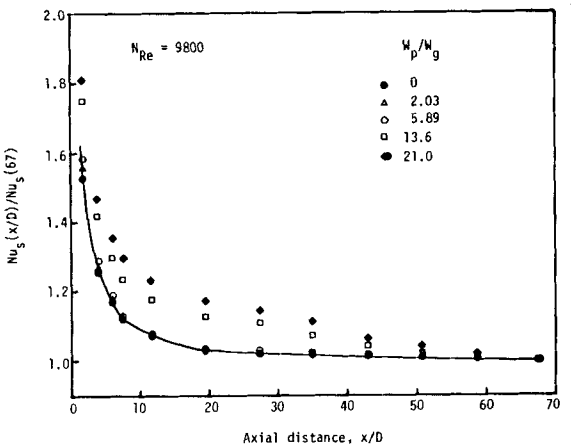

Figure 8. Effect of solids-loading ratio on thermal entry length, N_{Re} = 9,800.

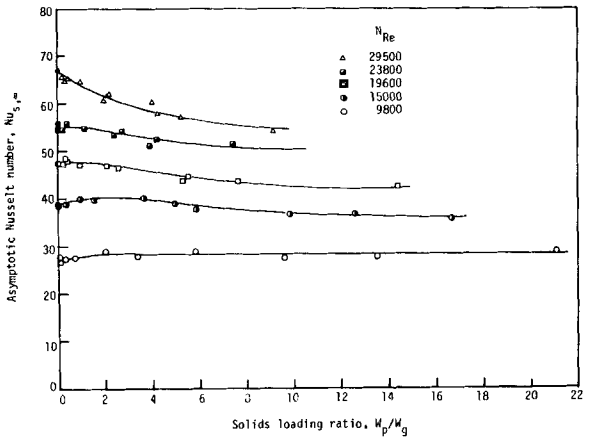

Figure 9. Effect of solids-loading ratio on asymptotic Nusselt number.

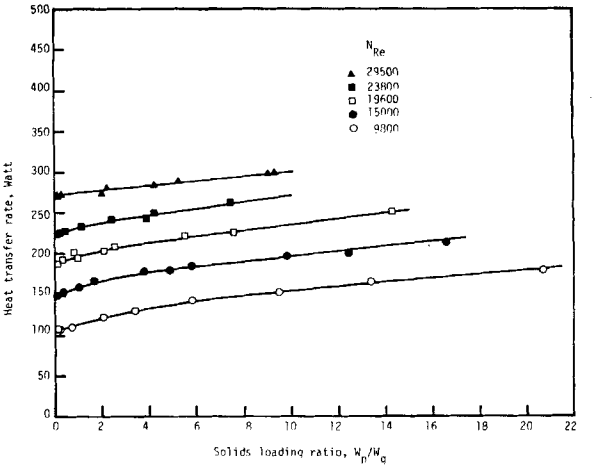

Figure 10. Effect of solids-loading ratio on heat transfer rate.

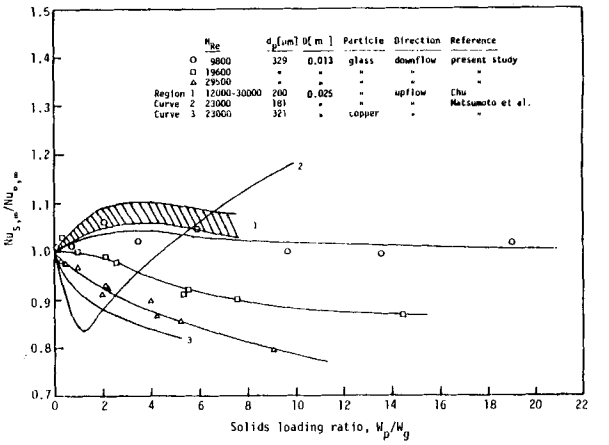

Figure 11. Comparison of Nusselt numbers in downflow with upflow data.

the entire axial distance. A possible cause for this behavior will be examined later in connection with the discussion of asymptotic Nusselt numbers. It is also seen that Nusselt number variations near the tube end are small even at the highest solids-loading ratio studied. Hence, the suspension Nusselt number at $x/D = 67$, Nu_s (67), may be safely assumed as an asymptotic value.

The results for a gas Reynolds number of 9,800 are plotted in terms of the ratio, $Nu_s(x/D)/Nu_s$ (67), in Figure 8, which illustrates that the thermal entry length is extended by the addition of particles. The reason for this is that particles experience a delay before following a temperature change in the surrounding gas. At the same loading ratio, the thermal entry length seems to depend on the gas Reynolds number, being extended more at higher gas Reynolds numbers.

The asymptotic Nusselt number for different values of gas Reynolds number is plotted against solids-loading ratio in Figure 9. At low gas Reynolds number, the Nusselt numbers are fairly constant for all solids-loading ratios covered, while at high Reynolds numbers, they decrease with increase in the loading ratio. Heat transfer to suspension flow is influenced by numerous interacting factors that are difficult to isolate. However, a plausible explanation for the opposite results observed in Figure 9 at low and high Reynolds numbers, may be given by considering promoting and inhibiting effects of particles in suspension heat transfer. An increase in heat transfer would result from penetration of the boundary layer by the particles and reduction of the boundary layer thickness. Conversely, particles may act as a resistance to radial heat transfer by reducing the turbulent eddy diffusivity near the wall due to slow response of particles to small eddies. As a result, these two effects might compensate each other at low gas Reynolds numbers, showing little change in the suspension Nusselt number over the entire range of ratios covered in this study. At high Reynolds numbers, however, the boundary layer becomes thinner, and the influence of the particle might be felt primarily through a resistance to radial heat transfer, resulting in a low Nusselt number. These different influences of particles on the suspension Nusselt number were also seen in Figure 7 where variations in Nusselt numbers in the entrance region with the solids-loading ratio followed reverse trends for the low and high gas Reynolds numbers.

In spite of decreasing or relatively constant Nusselt numbers with solids-loading ratio, the overall heat transfer rate to the suspension, as measured by the electrical power input for a fixed exit outside tube-wall temperature, was always greater than that for flow of gas alone at the same Reynolds number, as shown in Figure 10. This observation, reported also by other investigators (Depew, 1960; Chu, 1971; Matsumoto, 1978) who found that Nusselt numbers decreased upon the addition of particles, is due to the increased volumetric thermal capacity of the suspension flow.

Few data reported in the literature for upflow can be compared with the present results because of widely different experimental conditions, measurement techniques, and methods of analysis. Most workers have conducted experiments with small particles for which a dramatic change in heat transfer can be observed. In many works, Nusselt numbers are defined in terms of the suspension mixed-mean temperature, which is inadequate for coarse particles because of the large temperature difference between the phases. In Figure 11, the present data are compared with the upflow results of Chu (1971) and Matsumoto et al. (1978). Chu's data are based on a gas temperature calculated by assuming $Nu_p = 2$. Matsumoto et al. (1978) calculated the gas temperatures by assuming an analogy between temperature and velocity profiles that was expressed by a power-law formula. They also calculated Nusselt numbers on the

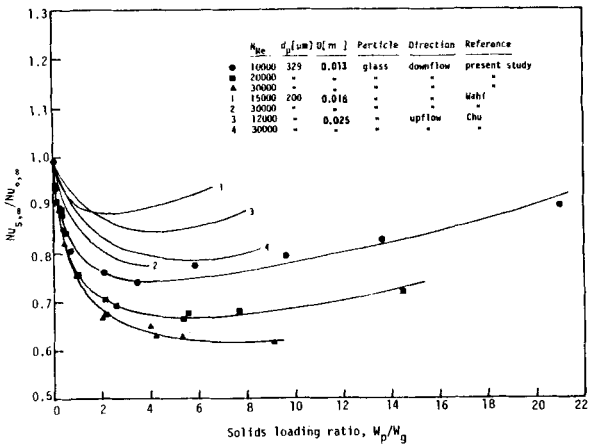

Figure 12. Comparison of Nusselt numbers based on the suspension mixed-mean temperature.

basis of the logarithmic terminal temperature difference. The trend shown by Chu's data is seen to be close to the present data for the gas Reynolds number of 9,800, but a large variation with the Reynolds number as found in this study does not appear in his data. Contrary to other results, the data of Matsumoto et al. for 181-μm glass beads show a complicated trend with a minimum Nusselt number at low solids-loading ratio, which is a general characteristic found for only fine particles. His results for larger 321-μm copper spheres however show a trend with loading ratio similar to the present study.

Local Nusselt numbers, as calculated on the basis of the suspension mixed-mean temperature using Eq. 8, are shown in Figure 12 where they are compared with the data of Wahi (1977) for downflow and Chu (1971) for upflow, which were analyzed in the same manner. Notice the great difference between the curves in Figures 11 and 12. For instance, in Figure 11, Nusselt numbers for the Reynolds number of 9,800 change little from the value for gas alone, while those in Figure 12 decrease rapidly by the addition of particles, reaching a minimum near a loading ratio of 3 to 4. The reason for the occurrence of minimum values observed in Figure 12 can be found clearly by referring to Figures 6 and 10 where the suspension mixed-mean temperature and overall heat transfer rate, respectively, are shown as a function of solids-loading ratio. These figures reveal that the minimum Nusselt number occurs due to a rapid decrease of the suspension mixed-mean temperature at low loadings and the relatively constant temperature at high loadings, while heat transfer rate increases steadily over the entire range of loadings. Although the present data fall on lower curves than others, the trend is similar for all studies in that the Nusselt number is larger at low Reynolds number than at high Reynolds number.

From the results shown in Figures 11 and 12, it is concluded that suspension Nusselt numbers in downflow are lower than those in upflow; but no quantitative comparison can be made because of uncertainty of the proper temperature driving force, limited data for only one particle size, and unaccountable differences between the data of different investigators.

ACKNOWLEDGMENT

This work was supported by the U.S. Department of Energy under contract No. E (49-18)-2006. The interest and assistance of W. H. Wiser and R. E. Wood are greatly appreciated.

NOTATION

A,B,C = constants in Eq. 6
C_{pg} = gas heat capacity
C_{pp} = particle heat capacity
d_p = particle diameter
D = tube diameter
E_p = particle holdup
h_p = particle heat transfer coefficient
k_g = gas thermal conductivity
N_{Pr} = Prandtl number, $C_{pg}\mu_g/k_g$
N_{Re} = Reynolds number, $DU_g\rho_g/\mu_g$
Nu_p = particle Nusselt number, hd_p/k_g
Nu_s = suspension Nusselt number based on the gas mixed-mean temperature, defined in Eq. 9
$Nu_{s,\infty}$ = asymptotic suspension Nusselt number
Nu_s' = suspension Nusselt number based on the suspension mixed-mean temperature, defined in Eq. 8
$Nu_{0,\infty}$ = asymptotic Nusselt number for single-phase flow
q_i = input heat flux
T_{gm} = gas mixed-mean temperature
T_{pm} = particle mixed-mean temperature
T_i = inlet temperature of suspension
T_{sm} = suspension mixed-mean temperature
T_{wi} = inside wall temperature of the tube
U_g = actual gas velocity
U_p = particle velocity
W_g = gas flow rate
W_p = particle flow rate
x = axial distance

LITERATURE CITED

Abel, W. T., D. E. Bluman, and J. P. O'Leary, "Gas-Solids Suspensions as Heat Carrying Mediums," ASME Paper No. 63-WA-210 (1963).
Boothroyd, R. G., "Heat Transfer in a Gas Borne Suspension of Fine Particles in Turbulent Duct Flow," *Appl. Sci. Res.*, **21**, 98 (1969).
Boothroyd, R. G., *Flowing Gas-Solids Suspensions*, Chapmann and Hall LTD, 11 New Fetter Lane, London (1971).
Briller, R., and R. L. Peskin, "Gas Solids Suspension Convective Heat Transfer at a Reynolds Number of 130000," *J. of Heat Transfer*, TRANS. ASME, Series C, **90**, 464 (1968).
Chu, N. C., "Turbulent Heat Transfer of Gas-Solid Two-Phase Flow in Circular Tubes," Ph.D. Thesis, University of Washington, Seattle, WA (1971).
Chu, N. C., and C. A. Depew, "Heat Transfer to Gas-Solids Suspension Flows in Vertical Circular Tubes," Proceedings of the 1972 Heat Transfer and Fluid Mechanics Institute, Northridge, CA, 371 (1972).
Depew, C. A., "Heat Transfer to Flowing Gas-Solids Mixtures in a Vertical Duct," Ph.D. Thesis, University of California, Berkeley (1960).
Depew, C. A., and L. Farber, "Heat Transfer to Pneumatically Conveyed Glass Particles of Fixed Size," *J. of Heat Transfer*, Trans. ASME, Series C, **85**, 164 (1963).
Depew, C. A., and T. J. Kramer, "Heat Transfer to Flowing Gas-Solids Mixtures," *Advances in Heat Transfer*, **9**, 113 (1973).
Farber, L., and C. A. Depew, "Heat Transfer Effects to Gas-Solids Mixture Using Solid Spherical Particles of Uniform Size," *Ind. Eng. Chem. Fund.*, **2**, 130 (1963).
Farber, L., and M. J. Morley, "Heat Transfer to Flowing Gas-Solids Mixtures in a Circular Tube," *Ind. Eng. Chem.*, **49**, 1143 (1957).
Kane, R. S., and R. Pfeffer, "Characteristics of Dilute Gas-Solids Suspensions in Drag Reducing Flow," NASA CR-2267 (1973).
Kays, W. M., and E. Y. Leung, "Heat Transfer in Annular Passages-Hydrodynamically Developed Turbulent Flow with Arbitrarily Prescribed Heat Flux," *Int. J. Heat Mass Transfer*, **6**, 537 (1963).
Kim, J. M., "Pressure Drop and Heat Transfer in Cocurrent Downflow of Gas-Solids Suspensions," Ph.D. Thesis, University of Utah, Salt Lake City, UT (1979).
Kreith, F., *Principles of Heat Transfer*, 3rd ed., Intext Educational Publishers, New York (1973).
Ladelfa, C. J., and M. I. Greene, "Economic Evaluation of Synthetic Natural Gas Production by Short Residence Time Hydropyrolysis of Coal," *Fuel Processing Technology*, **1**, 187 (1977/1978).
Massier, P. F., "A Forced-Convection and Nucleate-Boiling Heat Transfer Test Apparatus," JPL Technical Report No. 32-47 (1961).
Matsumoto, S., S. Ohnishi, and S. Maeda, "Heat Transfer to Vertical Gas-Solid Suspension Flows," *J. of Chem. Eng. of Japan*, **11**, No. 2, 89 (1978).
Ranz, W. E., and W. R. Marshall, Jr., "Evaporation from Drops," *Chem. Eng. Prog.*, **48**, 141 (1952).

Schluderberg, D. C., R. L. Whitelaw, and R. W. Carlson, "Gaseous Suspensions—A New Reactor Coolant," *Nucleonics*, **19**, 67 (1961).
Sparrow, E. M., T. M. Hallman, and R. S. Siegel, "Turbulent Heat Transfer in the Thermal Entrance Region of a Pipe with Uniform Heat Flux," *Appl. Sci. Res.*, Section A, **7**, 37 (1957).
Tien, C. L., "Heat Transfer by a Turbulently Flowing Fluid-Solids Mixture in a Pipe," *J. of Heat Transfer*, Trans. ASME, Series C, **83**, 183 (1961).
Tien, C. L., and V. Quan, "Local Heat Transfer Characteristics of Air-Glass and Air-Lead Mixtures in Turbulent Pipe Flow," ASME Paper No. 62-HT-15 (1962).
Wahi, M. K., "Heat Transfer to Flowing Gas-Solid Mixtures," *J. of Heat Transfer*, Trans. ASME, Series C, **99**, 145 (1977).
Wilkinson, G. T., and J. R. Norman, "Heat Transfer to a Suspension of Solids in a Gas," *Trans. Instn. Chem. Engrs.*, **45**, 314 (1967).
Wood, R. E., and W. H. Wiser, "Coal Liquefaction in Coiled Tube Reactors," *Ind. Eng. Chem. Process Des. Dev.*, **15**, 144 (1976).

Manuscript received June 16, 1981; revision received April 8, and accepted April 26, 1982.

Interfacial Area, Bubble Coalescence and Mass Transfer in Bubble Column Reactors

D. N. MILLER

Engineering Department
E. I. du Pont de Nemours and Co., Inc.
Wilmington, DE 19898

Relationships are developed for determining interfacial areas as a function of bubble coalescence and for predicting liquid-film-controlled mass transfer in deep seal bubble column reactors. Interfacial area is inversely dependent on mean bubble size; the mass transfer constant is directly dependent on bubble size. A correction for enhancement due to liquid-phase reaction must be applied, and enhancement is shown to decrease with increasing bubble size.

Experimental measurements on the catalyzed rate of oxygen absorption from air in aqueous sodium sulfite solutions were made in a 0.299 m diameter × 9.14 m high glass column. Water and aqueous solutions of a surfactant and corn syrup were used to simulate ranges of surface tensions, densities, and viscosities. Perforated plates with 0.00635-m holes and 2.85% open area were inserted at 1.524-m spacing on half of the experimental runs to show the effects of gas redispersion. Two-phase flow velocities were adjusted to cover ranges of interest in full-scale, commercial bubble column reactor design.

SCOPE

Reactions in which gas-liquid contacting is required for interphase mass transfer of a reactant are often carried out in deep seal bubble columns. Although reaction occurs in the liquid phase, the interphase mass transfer step is often a rate-limiting consideration in these systems.

The size requirement for reactors of this type is continually increasing, and reliable scale-up of performance from small-scale test data is a problem of ever-increasing importance.

Characterization of liquid-film-controlled mass transfer involves determination of two parameters: interfacial area a and the mass transfer constant k_L. Interfacial area decreases in deep seal contacting with increasing distance from the initial point of dispersion as bubble coalescence occurs. The overall mass transfer coefficient, which is the product $k_L a$, can decrease by an order of magnitude or more through a 10-m contacting zone as the result of bubble coalescence.

The mass transfer constant can be considerably enhanced over the value for purely physical absorption, where there is liquid-phase reaction. This effect increases with increasing reaction rate and is most pronounced when all the reaction occurs in the liquid film at the phase interface.

Two studies on the prediction of interfacial area and mass transfer in gas-liquid contacting have been reported in the recent literature (Bhavaraju, Russell and Blanch, 1978; Mersmann, 1979). Both are based on small-scale test work and are useful for relatively low two-phase holdup times. They do not, however, cover changes that occur with bubble coalescence as holdup times are extended in deep seal contracting.

Calderbank et al. (1962) studied bubble coalescence in a cross-flow contactor. A rectangular column 0.1016 × 0.1016 m square in cross section and 3 m high was used. Gas was sparged in at the bottom; and liquid fed uniformly through one side over the full column height and withdrawn through the opposite downstream side. With this system balanced for uniform flows, aeration and interfacial areas were measured by light transmittance and gamma ray radiation techniques. Bubble coalescence was found to follow a first-order rate dependence on bubble concentration.

This study was undertaken to develop design procedures for predicting mass transfer performance in bubble-column reactors with two-phase cocurrent upflow, which is the configuration most common in industrial practice.

CONCLUSIONS AND SIGNIFICANCE

A procedure has been developed for predicting liquid-film-controlled mass transfer in deep seal reactors where transfer of a reactant occurs between gas and liquid phase in cocurrent upflow.

Interfacial areas were found to be dependent on bubble coalescence which in turn follows a first-order dependence on bubble concentration. The first-order constant or frequency for bubble coalescence was correlated with two-phase velocity. The correlation has been developed for ranges of liquid-phase surface tensions, densities, and viscosities commonly found in